

# Divergence preserving interpolation on anisotropic quadrilateral meshes

Malte Braack<sup>a</sup>, Gert Lube<sup>b</sup>, Lars Röhe<sup>b</sup>

<sup>a</sup>Math. Dept., University of Kiel, D-24098, Germany

<sup>b</sup>Math. Dept., University of Göttingen, D-37083, Germany

---

## Abstract

For the solution of incompressible fluid models with inf-sup stable finite element pairs for velocity and pressure, interpolation operators are desirable which preserve the property of discrete zero divergence and enjoy the same local approximation properties as standard interpolation operators. Girault/Scott [21] constructed such an interpolator for the case of isotropic meshes. Here, we consider the existence of such an operator for special anisotropic meshes by combining their approach with results of Apel [1] on anisotropic interpolation on meshes of tensor-product type. Finally, we discuss the applicability of anisotropic grid resolution of boundary layers for incompressible turbulent flow problems.

*Keywords:* Anisotropic interpolation, incompressible flow, divergence preserving interpolation

---

## 1. Introduction

Interpolation operators are an important tool for the analysis of finite element schemes. For the solution of incompressible fluid models with inf-sup stable finite element pairs for velocity and pressure, interpolators are desirable which preserve the divergence constraint (3). Recently, such an interpolator had been constructed by Girault and Scott [21] for the case of isotropic (shape-regular) meshes. In practice, anisotropic meshes are used to represent complicated geometries and to resolve boundary layers for high Reynolds numbers flow. Then, appropriate interpolators should take the anisotropy of the mesh into account. The partial derivatives in the corresponding error estimates should be decoupled and weighted with the corresponding mesh sizes in the different spatial directions.

The construction of optimal anisotropic interpolators is a difficult task as the results of Apel/Matthies [3] show. They obtained optimal interpolation results with respect to the aspect ratio of the mesh only for very special non-conforming finite element pairs for velocity/pressure on meshes of tensor-product type, while the interpolation operator preserves the discrete divergence. In general, it is very likely that the aspect ratio of the mesh will influence the interpolation estimates.

Let  $\Omega \subset \mathbb{R}^d$ ,  $d \in \{2, 3\}$ , a domain with polygonal/polyhedral boundary and  $\mathbf{V} := H_0^1(\Omega)^d$  the corresponding Sobolev space of  $L^2$  functions with weak derivatives in  $L^2$  and vanishing traces on the boundary  $\partial\Omega$ . For a triangulation  $\mathbb{T}_h$  hexahedral cells of  $\Omega$ , the finite dimensional subspace  $\mathbf{V}_h \subset \mathbf{V}$  is the standard conforming finite element space of cellwise tensor-polynomials of maximal degree  $r \geq 0$ . For the theory of basic interpolation operators for finite elements, we refer to Ref. [15].

In the work of Apel ([5], Thm. 4.5), anisotropic linear interpolation operators  $\mathcal{A}_h$ , i.e.  $\mathcal{A}_h \in \mathcal{L}(\mathbf{V}; \mathbf{V}_h)$ , are constructed on tensor-product meshes (see Section 2) with the interpolation property on all cells  $K \in \mathbb{T}_h$ :

$$|\mathbf{v} - \mathcal{A}_h \mathbf{v}|_{H^m(K)}^2 \lesssim \sum_{|\alpha|=l-m} h_K^{2\alpha} |D^\alpha \mathbf{v}|_{H^m(\omega(K))}^2 \quad \forall \mathbf{v} \in H^l(\omega(K))^d, \quad (1)$$

---

*Email addresses:* braack@math.uni-kiel.de (Malte Braack), lube@math.uni-goettingen.de (Gert Lube), roehe@math.uni-goettingen.de (Lars Röhe)

with  $0 \leq m \leq l$ ,  $1 \leq l \leq r + 1$ . The expressions  $h^\alpha$  and  $D^\alpha$  for  $\alpha \in \mathbb{N}^d$  are the usual multi-index notations. Here we use the expression  $a \lesssim b$  for  $a \leq Cb$  with a  $h$ -independent constant  $C$ . Moreover,  $\omega(K)$  is the patch of all cells  $K'$  having a common edge/face with element  $K$ . Please note that estimate (1) is still valid on  $H^1(\Omega)$ . Moreover, from Thm. 9 of Ref. [1] we have the existence of an operator  $\mathcal{A}_h$  for channel geometries, preserving homogeneous Dirichlet conditions on long edges/faces. The construction of the operator  $\mathcal{A}_h$  is based on the the work of Scott and Zhang [27].

In this paper, we will construct a similar operator  $P_h \in \mathcal{L}(\mathbf{V}; \mathbf{V}_h)$  on special Cartesian anisotropic meshes which also fulfills the (potentially non-optimal) anisotropic interpolation property

$$\|\mathbf{v} - P_h \mathbf{v}\|_{L^2(K)}^2 + h_{d,K}^2 \|\mathbf{v} - P_h \mathbf{v}\|_{H^1(K)}^2 \lesssim \frac{1}{\gamma_i^2} \sum_{|\alpha|=l} h^{2\alpha} \|D^\alpha \mathbf{v}\|_{L^2(\omega(K))}^2 \quad (2)$$

where  $h_{d,k}$  denotes the shortest edge of element  $K$  and  $\gamma_i$  is the maximal aspect ratio of a patch  $\omega(K)$  containing  $K$ . Such kind of interpolation property for anisotropic meshes had been observed by others too, e.g. in Refs. [11, 19]. Following Girault and Scott [21], we will show that the operator additionally preserves the discrete divergence in the sense

$$(q_h, \operatorname{div}(P_h \mathbf{v} - \mathbf{v})) = 0 \quad \forall \mathbf{v} \in \mathbf{V} \quad \forall q_h \in Q_h, \quad (3)$$

for inf-sup stable function spaces  $\mathbf{V}_h$ ,  $Q_h$ , where  $Q_h$  is a discrete subspace of

$$Q := L_*^2(\Omega) := \left\{ q \in L^2(\Omega) \mid \int_{\Omega} q dx = 0 \right\}.$$

The main result of this paper is given in Theorem 3.5. Finally, for the lowest order Taylor-Hood element in the planar case, we discuss the size of the parameter  $\gamma_i$ , see Theorem 4.1.

This paper is organized as follows. All notations and assumptions are given in the next Section 2. The anisotropic, divergence preserving interpolation operator  $P_h$  will be constructed in Section 3. An essential ingredient is the availability of a local inf-sup condition which may depend on aspect ratios. As an example, we consider in Section 4 such a dependence in the particular case of the lowest order Taylor-Hood element in the planar case  $d = 2$ . Finally, in Section 6, we will apply the theoretical results to incompressible flow problems.

## 2. Preliminaries

In this work we consider tensor-product meshes  $\mathbb{T}_h$  in  $d \in \{2, 3\}$  dimensions where the transformation from reference cell  $\hat{K} = (-1, 1)^d$  to another cell  $K \in \mathbb{T}_h$  can be described by the transformation

$$x = \operatorname{diag}(h_{1,K}, \dots, h_{d,K}) \hat{x} + a_K$$

with the local mesh sizes  $h_{i,K}$  into direction  $i$  and a shift  $a_K \in \mathbb{R}^d$ . The analysis requires further restrictions on the mesh which holds for many applications, e.g. for the geometry of a channel flow (possibly after changing the order of the coordinates):

**Assumption 1.** *The mesh size in direction  $d$  is locally the smallest one,*

$$h_{d,K} \leq h_{i,K} \quad \forall i \in \{1, \dots, d-1\},$$

*whereas the mesh sizes in the remaining directions are isotropic. Moreover, we demand that there is no abrupt change in the element sizes of neighboring cells,*

$$h_{i,K'} \lesssim h_{i,K} \lesssim h_{i,K'} \quad \forall K, K' \in \mathbb{T}_h, \bar{K}' \cap \bar{K} \neq \emptyset.$$

The second assumption is related to the set of all inner edges (and boundary edges without Dirichlet conditions), denoted by  $\mathcal{E}_h$ . For every  $K \in \mathbb{T}_h$  we define a 'unique' long edge:

ass:2

**Assumption 2.** *There is an injective map*

$$\varepsilon_h: \mathbb{T}_h \rightarrow \mathcal{E}_h,$$

with the following property:

$$h_{1,K} \lesssim |\varepsilon_h(K)| \lesssim h_{1,K} \quad \forall K \in \mathbb{T}_h.$$

The specific choice of the map  $\varepsilon_h$  for certain model configurations will be presented in Section 5. The space of all polynomials on  $\hat{K}$  with maximal degree  $r \in \mathbb{N}$  in each coordinate direction is denoted by  $\mathbb{Q}_r(\hat{K})$ . We will use the continuous  $H^1$ -conforming finite element space

$$\mathbb{Q}_{h,r} := \left\{ v_h \in H^1(\Omega) \mid v_h|_K \circ F_K \in \mathbb{Q}_r(\hat{K}) \quad \forall K \in \mathbb{T}_h \right\}.$$

For incompressible models, we apply the continuous and discrete spaces

$$\begin{aligned} \mathbf{V} &:= H^1(\Omega)^d \quad \text{and} \quad \mathbf{V}_h := \mathbf{V} \cap \mathbb{Q}_{h,r}^d \\ Q &:= L^2(\Omega) \quad \text{and} \quad Q_h := Q \cap \mathbb{Q}_{h,s}. \end{aligned}$$

without Dirichlet conditions. Later on, we also treat the case of Dirichlet conditions. Henceforth, the norm of the Sobolev space  $H^l(D)$ ,  $D \subset \Omega$  with  $l \in \mathbb{N}_0$  will be denoted by  $\|\cdot\|_{l,D}$ . In case of  $l = 0$ , we usually simply write  $\|\cdot\|_D$ .

For the description of anisotropic meshes, we take advantage of the standard multiindex notation

$$h^\alpha = \prod_{i=1}^d h_{i,K}^{\alpha_i} \quad \text{and} \quad D^\alpha = \prod_{i=1}^d \partial_i^{\alpha_i}.$$

Furthermore,  $\omega(K) \subset \Omega$  denotes the neighborhood of  $K$ , i.e. a patch of cells surrounding  $K \in \mathbb{T}_h$ . Henceforth we will use different variants of  $\omega(K)$ .

In the analysis below, we apply the following technical results.

**Lemma 2.1.** *It holds for  $d \in \{2, 3\}$  on tensor-product meshes fulfilling Assumption 1:*

$$\int_{\partial K} |\mathbf{v}_h| ds \lesssim \left( \frac{h_{1,K}}{h_{2,K} \cdots h_{d,K}} \right)^{1/2} \|\mathbf{v}_h\|_K \quad \forall \mathbf{v}_h \in \mathbf{V}_h.$$

*Proof.* By transformation back and forth to the reference element, and due to norm equivalence on finite dimensional spaces we obtain

$$\begin{aligned} \int_{\partial K} |\mathbf{v}_h| ds &= \sum_{e \in \partial K} h_e \int_{\hat{e}} |\hat{\mathbf{v}}_h| ds \\ &\lesssim h_{1,K} \left( \int_{\hat{K}} \hat{\mathbf{v}}_h^2 dx \right)^{1/2} \\ &= h_{1,K} |K|^{-1/2} \left( \int_K \mathbf{v}_h^2 dx \right)^{1/2} \\ &= \left( \frac{h_{1,K}}{h_{2,K} \cdots h_{d,K}} \right)^{1/2} \|\mathbf{v}_h\|_K. \end{aligned}$$

□

**Lemma 2.2.** *Let  $\mathbf{v} \in H^1(K) \cap C^1(K)$  with  $\int_K \mathbf{v} dx = 0$  and a domain  $K \subset \mathbb{R}^d$  convex and bounded. Then it holds*

$$\|\mathbf{v}\|_K \lesssim \left( \sum_{r=1}^d h_{r,K}^2 \left\| \frac{\partial \mathbf{v}}{\partial x_r} \right\|_K^2 \right)^{1/2}.$$

*Proof.* The assertion is a simple consequence of transformation onto the reference element, application of the isotropic Poincaré's inequality (see [18] pp.105) and inverse transformation. □

construction

### 3. Construction of the operator

In this section we will construct and show the existence of an operator  $P_h \in \mathcal{L}(\mathbf{V}; \mathbf{V}_h)$  fulfilling a variant of (1) and preserves the discrete divergence (3), under certain assumptions. To this goal, we will take a basic anisotropic interpolation operator  $\mathcal{A}_h$ , e.g. from Ref. [5], and modify it to finally obtain the desired properties in Theorem 3.5.

As a first step we have to prove the existence of operators which fulfill an interpolation property and preserve the discrete divergence tested against piecewise constant functions, see Lemma 3.3 below. With this in mind we prove the following lemma.

**Lemma 3.1** (Stability). *Let  $d \in \{2, 3\}$  and  $r \geq 2$  and the triangulation  $\mathbb{T}_h$  fulfills Assumptions 1 and 2. Then there exists an operator  $L_h \in \mathcal{L}(\mathbf{V}, \mathbf{V}_h)$  such that the following properties are fulfilled for every function  $\mathbf{v} \in \mathbf{V}$ :*

(i) *The discrete divergence is preserved when tested against a piecewise constant function,*

$$\int_K \operatorname{div}(\mathbf{v} - L_h \mathbf{v}) dx = 0.$$

(ii) *The operator is locally stable with respect to the  $L^2$ -norm, i.e.*

$$\|L_h \mathbf{v}\|_K \lesssim \|\mathbf{v}\|_{\omega(K)}.$$

(iii) *The partial derivatives in each direction are locally stable, i.e.*

$$\|\partial_{x_i} L_h \mathbf{v}\|_K \lesssim h_{i,K}^{-1} \|\mathbf{v}\|_{\omega(K)}$$

for every  $i \in \{1, \dots, d\}$ .

*Proof.* The first step is the construction of the operator. For each  $K \in \mathbb{T}_h$  the assigned long edge according to Assumption 2 is  $\bar{\varepsilon}_h(K) \in \mathcal{E}_h$ . Since  $r \geq 2$  there is a bubble function in  $\mathbf{V}_h$  assigned to  $\varepsilon_h(K)$  denoted by  $\varphi_{\varepsilon_h(K)} \in \mathbf{V}_h$ . The support of this bubble function consists of two cells, and we present an example of the support indicated by the grey area in Figure 2. Additionally, we can assume that these bubble functions are normalized in the sense

$$\int_{\partial K'} \varphi_{\varepsilon_h(K)} \cdot n ds = \delta_{K',K},$$

with the Kronecker symbol  $\delta_{K',K}$  for two cells  $K', K$ . Then we set

$$e_K(\mathbf{v}) := \int_{\partial K} \mathbf{v} \cdot n ds \quad \text{and} \quad L_h \mathbf{v} := \sum_{K \in \mathbb{T}_h} e_K(\mathbf{v}) \cdot \varphi_{\varepsilon_h(K)}.$$

The well-posedness and linearity of  $L_h : \mathbf{V} \rightarrow \mathbf{V}_h$  is obvious due to the construction. We now show the properties (i)-(iii). The conservation of divergence (i) can be shown by integration by parts:

$$\begin{aligned} \int_{K'} \operatorname{div} L_h \mathbf{v} dx &= \int_{\partial K'} L_h \mathbf{v} \cdot n ds \\ &= \int_{\partial K'} \sum_{K \in \mathbb{T}_h} e_K(\mathbf{v}) \varphi_{\varepsilon_h(K)} \cdot n ds \\ &= \sum_{K \in \mathbb{T}_h} e_K(\mathbf{v}) \int_{\partial K'} \varphi_{\varepsilon_h(K)} \cdot n ds \\ &= \int_{\partial K'} \mathbf{v} \cdot n ds \\ &= \int_{K'} \operatorname{div} \mathbf{v} dx. \end{aligned}$$

For proving the stability estimate (ii) we use the definition of  $L_h$  and obtain

$$\begin{aligned} \|L_h \mathbf{v}\|_K^2 &= \int_K \left( \sum_{K^* \in \mathbb{T}_h} e_{K^*}(\mathbf{v}) \cdot \varphi_{\varepsilon_h(K^*)} \right)^2 dx \\ &\leq |e_K(\mathbf{v})|^2 \|\varphi_{\varepsilon_h(K)}\|_K^2 + |e_{K'}(\mathbf{v})|^2 \|\varphi_{\varepsilon_h(K')}\|_{K'}^2. \end{aligned}$$

Here we used also that  $\text{supp}(\varphi_{\varepsilon_h(K)})$  only contains two cells denoted by  $K'$  and  $K$  itself. The functions  $\varphi_{\varepsilon_h(K)}$  are defined on long edges like in Assumption 2, which is why the integral over this edge scales like the edge itself, i.e.

$$\|\varphi_{\varepsilon_h(K)}\|_K^2 \lesssim \int_K h_{1,K}^{-2} dx \lesssim \frac{h_{2,K} \cdots h_{d,K}}{h_{1,K}}$$

for every  $K \in \mathbb{T}_h$ . Now it is left to estimate  $|e_K(\mathbf{v})|^2$ , i.e.  $|\int_{\partial K} \mathbf{v} \cdot n ds|$ . Since the normal  $n$  has length 1, Lemma 2.1 provides

$$\|L_h \mathbf{v}\|_K^2 \lesssim \|\mathbf{v}\|_K^2 + \|\mathbf{v}\|_{K'}^2 \lesssim \|\mathbf{v}\|_{\omega(K)}^2.$$

For showing (iii) we apply an inverse inequality ([2], Remark 3.6) in each direction and use (ii)

$$\|\partial_{x_i} L_h \mathbf{v}\|_K \lesssim h_{i,K}^{-1} \|L_h \mathbf{v}\|_K \lesssim h_{i,K}^{-1} \|\mathbf{v}\|_{\omega(K)} \quad \forall i \in \{1, \dots, d\}.$$

□

Let  $\mathcal{A}_h \in \mathcal{L}(\mathbf{V}, \mathbf{V}_h)$  be an interpolation operator, where for  $m \in \{0, 1\}$

$$|\mathbf{v} - \mathcal{A}_h \mathbf{v}|_{m,K}^2 \lesssim \sum_{|\alpha|=r+1-m} h_K^{2\alpha} |D^\alpha \mathbf{v}|_{m,\omega(K)}^2 \quad (4) \quad \text{eq:interpol}$$

is fulfilled for every  $\mathbf{v} \in H^l(\Omega)$ . The existence of such an operator  $\mathcal{A}_h$  is shown e.g. in [5] (denoted there by  $E_h$ ).

**Corollary 3.2.** *Let  $r \geq 2$  and the triangulation  $\mathbb{T}_h$  is assumed to fulfill Assumptions 1 and 2. Let  $\mathcal{A}_h \in \mathcal{L}(\mathbf{V}, \mathbf{V}_h)$  be an operator with property (4). Then there exists a related operator  $\tilde{L}_h \in \mathcal{L}(\mathbf{V}, \mathbf{V}_h)$  with*

$$\int_K \text{div} \tilde{L}_h \mathbf{v} dx = \int_K \text{div}(\mathbf{v} - \mathcal{A}_h \mathbf{v}) dx \quad \forall \mathbf{v} \in \mathbf{V} \quad \forall K \in \mathbb{T}_h, \quad (5) \quad \text{eq:divLA}$$

and with  $0 \leq l \leq r+1$  the stability properties for every  $\mathbf{v} \in \mathbf{V}$  and every  $K \in \mathbb{T}_h$ :

$$\|\tilde{L}_h \mathbf{v}\|_K^2 + h_{i,K}^2 \|\partial_{x_i} \tilde{L}_h \mathbf{v}\|_K^2 \lesssim \sum_{|\alpha|=l} h_K^{2\alpha} \|D^\alpha \mathbf{v}\|_{\omega(K)}^2 \quad 1 \leq i \leq d,$$

with a (larger) patch  $\omega(K)$  of elements surrounding  $K$ .

*Proof.* We set  $\tilde{L}_h := L_h \circ (id - \mathcal{A}_h)$ , where  $L_h$  is the operator of Lemma 3.1. The equality (5) follows by

$$\int_K \text{div} \tilde{L}_h \mathbf{v} dx = \int_K \text{div} L_h \mathbf{v} dx - \int_K \text{div} L_h \mathcal{A}_h \mathbf{v} dx = \int_K \text{div}(\mathbf{v} - \mathcal{A}_h \mathbf{v}) dx.$$

The stability estimates follow via  $L^2$ -stability of  $L_h$  in Lemma 3.1 and the interpolation property (4) of  $\mathcal{A}_h$ :

$$\|\tilde{L}_h \mathbf{v}\|_K^2 \lesssim \|\mathbf{v} - \mathcal{A}_h \mathbf{v}\|_{\omega(K)}^2 \lesssim \sum_{|\alpha|=l} h_K^{2\alpha} \|D^\alpha \mathbf{v}\|_{\omega(K)}^2.$$

The stability of the derivatives follows now by an inverse estimate:

$$\|\partial_{x_i} \tilde{L}_h \mathbf{v}\|_K \lesssim h_{i,K}^{-1} \|\tilde{L}_h \mathbf{v}\|_K.$$

□

Now we are in the situation to construct an anisotropic interpolation operator which preserves the divergence at least on each cell:

**Lemma 3.3.** *Let  $r \geq 2$  and the triangulation  $\mathbb{T}_h$  fulfill Assumptions 1 and 2. Then there is an operator  $\Pi_h : \mathbf{V} \rightarrow \mathbf{V}_h = [\mathbb{Q}_{h,r}]^d$ , such that*

(i) *for every  $K \in \mathbb{T}_h$  and every  $\mathbf{v} \in [H^1(\Omega)]^d$*

$$\int_K \operatorname{div}(\mathbf{v} - \Pi_h \mathbf{v}) \, dx = 0$$

(ii) *Approximability for every  $\mathbf{v} \in [H^1(\Omega)]^d$ :*

$$\begin{aligned} \|\mathbf{v} - \Pi_h \mathbf{v}\|_K^2 &\lesssim \sum_{|\alpha|=l} h_K^{2\alpha} \|D^\alpha \mathbf{v}\|_{\omega(K)}^2, \\ |\mathbf{v} - \Pi_h \mathbf{v}|_{1,K}^2 &\lesssim \sum_{|\alpha|=l-1} h_K^{2\alpha} |D^\alpha \mathbf{v}|_{1,\omega(K)}^2 + h_{d,K}^{-2} \sum_{|\alpha|=l} h_K^{2\alpha} \|D^\alpha \mathbf{v}\|_{\omega(K)}^2. \end{aligned}$$

*Proof.* We apply Corollary 3.2 and set  $\Pi_h := \mathcal{A}_h + \tilde{L}_h$ . With this definition (i) is straight forward. The  $L^2$ -estimate follows also directly due to (4) and Corollary 3.2. The second estimate in (ii) follows by

$$\begin{aligned} |\mathbf{v} - \Pi_h(\mathbf{v})|_{1,K}^2 &\leq |\mathbf{v} - \mathcal{A}_h \mathbf{v}|_{1,K}^2 + \|\nabla \tilde{L}_h \mathbf{v}\|_K^2 \\ &= |\mathbf{v} - \mathcal{A}_h \mathbf{v}|_{1,K}^2 + \sum_{i=1}^d \|\partial_{x_i} \tilde{L}_h \mathbf{v}\|_K^2. \end{aligned}$$

□

**Remark 3.4.** *Since the injective map  $\varepsilon_h$  only maps on inner edges, the correction  $\tilde{L}_h$  has no influence on the values on the boundary. As a consequence,  $\Pi_h$  preserves Dirichlet boundary conditions on those parts of the boundary, where  $\mathcal{A}_h$  preserved them.*

Using this result, we will show the existence of an operator with the desired properties (2) and (3). But before starting the proof, we define the spaces we will use, following [21, 20]. For the given pair  $(\mathbf{V}_h, Q_h)$  of finite element spaces, we define for each function  $q_h \in Q_h$  and each  $K \in \mathbb{T}_h$

$$\tau(q_h)|_K = q_h - \frac{1}{|K|} \int_K q_h \, dx$$

and set

$$\tilde{Q}_h := \{\tau(q_h) \mid q_h \in Q_h\}.$$

The functions in  $\tilde{Q}_h$  are piecewise polynomial of the same degree as the functions in  $Q_h$ , but  $\tilde{Q}_h$  is not necessarily a subspace of  $Q_h$ . For the velocities we define the space

$$\tilde{\mathbf{V}}_h := \left\{ \mathbf{v}_h \in \mathbf{V}_h \mid \int_K \operatorname{div} \mathbf{v}_h \, dx = 0 \, \forall K \in \mathbb{T}_h \right\}$$

and also local variants of both spaces for macro-elements  $M$ ,

$$\begin{aligned} \tilde{\mathbf{V}}_h(M) &:= \left\{ \mathbf{v}_h \in \tilde{\mathbf{V}}_h \mid \operatorname{supp}(\mathbf{v}_h) \subset M \right\}, \\ \tilde{Q}_h(M) &:= \left\{ \tilde{q}_h|_M \mid \tilde{q}_h \in \tilde{Q}_h \right\}. \end{aligned}$$

For our partition of macro-elements  $\{M_i\}_{i=1}^R$  with  $\bar{\Omega} = \cup_{i=1}^R M_i$  we will assume that each  $M_i$  is connected and the union of finitely many cells  $K \in \mathbb{T}_h$ . Furthermore  $M_i \neq M_j$  for  $i \neq j$  has to hold true, even if we allow the macro-elements to intersect. We only assume that each  $K$  only belongs to a bounded number of macro-elements, which is independent of  $h$ . The following assumption is known as Hypothesis H.4 in [20] (Section II.1.4).

**Assumption 3.** *There is a set of macro elements  $\{M_i\}_{i=1}^R$  defined as above and constants  $\gamma_i$  possibly depending on the aspect ratio of the macro-element  $M_i$  such that*

$$\inf_{q_h \in \tilde{Q}_h(M_i)} \sup_{\mathbf{v}_h \in \tilde{\mathbf{V}}_h(M_i)} \frac{(q_h, \operatorname{div} \mathbf{v}_h)_{M_i}}{\|q_h\|_{M_i} \|\nabla \mathbf{v}_h\|_{M_i}} \geq \gamma_i. \quad (6)$$

**Theorem 3.5.** *Under the Assumptions 1, 2, 3 there exists an operator  $P_h \in \mathcal{L}(\mathbf{V}, \mathbf{V}_h)$  satisfying*

$$(q_h, \operatorname{div} (P_h \mathbf{v} - \mathbf{v})) = 0 \quad \forall \mathbf{v} \in \mathbf{V} \quad \forall q_h \in Q_h, \quad (7)$$

$$\|\mathbf{v} - P_h \mathbf{v}\|_K^2 + h_{d,K}^2 |\mathbf{v} - P_h \mathbf{v}|_{1,K}^2 \lesssim \frac{1}{\gamma_i^2} \sum_{|\alpha|=l} h_K^{2\alpha} \|D^\alpha \mathbf{v}\|_{\omega(K)}^2 \quad (8)$$

for  $K \subset M_i$ .

*Proof.* First let us give an outline of the proof. We will extend the operator  $\Pi_h$  of Lemma 3.3 by a correction  $\mathbf{C}_h$ , which we get from the local inf-sup condition (6). Then we define

$$P_h := \Pi_h + \mathbf{C}_h.$$

Therefore, in step (i) we will show the construction of  $\mathbf{C}_h$ , show an interpolation property of  $\mathbf{C}_h$  in step (ii) and conclude with (iii) by putting everything together.

Step (i): Since the macro-elements may overlap, we first define a non-overlapping partition of macro-elements  $\{\tilde{M}_i\}_{i=1}^R$  associated to the original partition  $\{M_i\}_{i=1}^R$ . We set  $\tilde{M}_1 = M_1$ , denote by  $\tilde{M}_2$  the union of elements  $K \subseteq M_2$  and  $K \not\subseteq M_1$ . In general,

$$\tilde{M}_i = \bigcup_{K \in \mathbb{T}_h, K \subseteq N_i} K, \quad \text{with } N_i := M_i \setminus \left( M_i \cap \bigcup_{j=1}^{i-1} \tilde{M}_j \right).$$

With this construction the  $\tilde{M}_i$  are pairwise disjoint. If a  $\tilde{M}_i$  is empty, we can simply omit it, while we still have the property

$$\Omega = \bigcup_{i=1}^R \tilde{M}_i \quad \text{with } \tilde{M}_i \subseteq M_i \text{ for } 1 \leq i \leq R.$$

Let  $\mathbf{v} \in \mathbf{V}$  be given. The local inf-sup condition (6) implies that for each patch  $M_i$  there exists a unique function  $\mathbf{c}_{h,i} \in \tilde{\mathbf{V}}_h^\perp(M_i)$  (depending on  $\mathbf{v}$ ) with

$$(q_h, \operatorname{div} \mathbf{c}_{h,i})_{M_i} = (q_h, \operatorname{div} (\mathbf{v} - \Pi_h \mathbf{v}))_{\tilde{M}_i} \quad \forall q_h \in \tilde{Q}_h(M_i), \quad (9)$$

where

$$\begin{aligned} \tilde{\mathbf{V}}_h^{\operatorname{div}}(M) &:= \left\{ \mathbf{v}_h \in \tilde{\mathbf{V}}_h(M) \mid (q_h, \operatorname{div} \mathbf{v}_h)_M = 0 \quad \forall q_h \in \tilde{Q}_h(M) \right\} \\ \tilde{\mathbf{V}}_h^\perp(M) &:= \left\{ \mathbf{v}_h \in \tilde{\mathbf{V}}_h(M) \mid (\nabla \mathbf{v}_h, \nabla \mathbf{w}_h)_M = 0 \quad \forall \mathbf{w}_h \in \tilde{\mathbf{V}}_h^{\operatorname{div}}(M) \right\}. \end{aligned}$$

Then we extend each  $\mathbf{c}_{h,i}$  by zero outside  $M_i$  and set

$$\mathbf{C}_h \mathbf{v} := \sum_{i=1}^R \mathbf{c}_{h,i}.$$

Due to the construction we obtain  $\mathbf{C}_h \mathbf{v} \in \widetilde{\mathbf{V}}_h$  and for all  $q_h \in Q_h$ :

$$\begin{aligned} (q_h, \operatorname{div} \mathbf{C}_h \mathbf{v})_\Omega &= \sum_{i=1}^R (q_h, \operatorname{div} \mathbf{c}_{h,i})_\Omega \\ &= \sum_{i=1}^R (q_h, \operatorname{div} \mathbf{c}_{h,i})_{M_i} \\ &= \sum_{i=1}^R (q_h, \operatorname{div} (\mathbf{v} - \Pi_h \mathbf{v}))_{\widetilde{M}_i} \\ &= (q_h, \operatorname{div} (\mathbf{v} - \Pi_h \mathbf{v}))_\Omega. \end{aligned}$$

Due to this construction,  $\mathbf{C}_h$  is a linear operator.

Step (ii): The local inf-sup condition (6) implies the existence of a discrete pressure  $q_h \in \widetilde{Q}_h(M_i)$ , so that:

$$(q_h, \operatorname{div} \mathbf{c}_{h,i}) \geq \gamma_i \|\nabla \mathbf{c}_{h,i}\|_{M_i} \|q_h\|_{M_i},$$

where  $\gamma_i$  possibly depends on the aspect ratio of the macro-element  $M_i$ . Due to the property (9) of  $\mathbf{c}_{h,i}$  and due to  $M_i \subset \widetilde{M}_i$  it follows

$$\begin{aligned} \|\nabla \mathbf{c}_{h,i}\|_{M_i} &\leq (\gamma_i \|q_h\|_{M_i})^{-1} (q_h, \operatorname{div} (\mathbf{v} - \Pi_h \mathbf{v}))_{\widetilde{M}_i} \\ &\leq \gamma_i^{-1} \|\operatorname{div} (\mathbf{v} - \Pi_h \mathbf{v})\|_{\widetilde{M}_i}, \end{aligned}$$

Since  $\mathbf{c}_{h,i} \in H_0^1(M_i)$  for each  $i$ , the functions  $\mathbf{c}_{h,i}$  have vanishing traces on  $\partial M_i$ . Hence, the Friedrichs inequality ([18], p. 55) and Assumption 1 gives an interpolation property for each  $\mathbf{c}_{h,i}$ :

$$\begin{aligned} \|\mathbf{c}_{h,i}\|_{M_i} &\lesssim h_{d,K_i} \|\nabla \mathbf{c}_{h,i}\|_{M_i} \\ &\leq \frac{h_{d,K_i}}{\gamma_i} \|\operatorname{div} (\mathbf{v} - \Pi_h \mathbf{v})\|_{\widetilde{M}_i}, \end{aligned}$$

with arbitrary elements  $K_i \in \mathbb{T}_h$ ,  $K_i \subset M_i$ . In the next step, we will extend the property to  $\mathbf{C}_h$ . Let us point out that due to the construction  $\mathbf{c}_{h,M_i}$  vanishes outside  $M_i$  and  $M_i$  only intersects with a bounded number of other macro-elements. Let us call this number  $\mu$  and obtain for some new indices  $j \leq R_i \leq \mu \leq R$

$$\|\mathbf{C}_h \mathbf{v}\|_{M_i}^2 = \int_{M_i} \left| \sum_{j=1}^{R_i} \mathbf{c}_{h,j} \right|^2 \leq \mu \int_{M_i} \sum_{j=1}^{R_i} |\mathbf{c}_{h,j}|^2 \leq \mu \sum_{j=1}^{R_i} \|\mathbf{c}_{h,j}\|_{M_i \cap M_j}^2 \leq \mu h_{d,K_i}^2 \sum_{j=1}^{R_i} \|\nabla \mathbf{c}_{h,j}\|_{M_i \cap M_j}^2.$$

A similar estimate for the gradient leads us to

$$\begin{aligned} \|\mathbf{C}_h \mathbf{v}\|_{M_i} + h_{d,K_i} \|\nabla \mathbf{C}_h \mathbf{v}\|_{M_i} &\lesssim h_{d,K} \gamma_i^{-1} \|\operatorname{div} (\mathbf{v} - \Pi_h \mathbf{v})\|_{\omega(M_i)} \\ &\lesssim h_{d,K_i} \gamma_i^{-1} |\mathbf{v} - \Pi_h \mathbf{v}|_{1,\omega(M_i)}, \end{aligned}$$

where  $\omega(M_i)$  is the union of all  $\widetilde{M}_j$  such that  $M_i$  and  $M_j$  intersect.

Step (iii): Due to the interpolation property of the operator  $\Pi_h$  in Lemma 3.3 and due to  $\gamma_i \leq 1$ , it is sufficient for the interpolation property of  $P_h$  to have a proper bound on

$$\|\mathbf{C}_h \mathbf{v}\|_K^2 + h_{d,K}^2 \|\nabla \mathbf{C}_h \mathbf{v}\|_K^2,$$



for an arbitrary cell  $K \in \mathbb{T}_h$ . Let  $i$  be the index so that  $K \subset M_i$  and  $\omega(K)$  a sufficiently large patch with  $\omega(M_i) \subset \omega(K)$ . With help of the local estimate shown in (ii) we conclude

$$\begin{aligned} \|\mathbf{C}_h \mathbf{v}\|_K^2 + h_{d,K}^2 \|\nabla \mathbf{C}_h \mathbf{v}\|_K^2 &\lesssim h_{d,K}^2 \gamma_i^{-2} |\mathbf{v} - \Pi_h \mathbf{v}|_{1,\omega(M_i)}^2 \\ &\lesssim \gamma_i^{-2} \left( \sum_{|\alpha|=l-1} h_{d,K}^2 h^{2\alpha} |D^\alpha \mathbf{v}|_{1,\omega(K)}^2 + \sum_{|\alpha|=l} h^{2\alpha} \|D^\alpha \mathbf{v}\|_{\omega(K)}^2 \right) \\ &\leq \gamma_i^{-2} \sum_{|\alpha|=l} h^{2\alpha} \|D^\alpha \mathbf{v}\|_{\omega(K)}^2 . \end{aligned}$$

This finishes the proof.  $\square$

Let us point out that such an operator does not exist for every finite element, since one can prove inf-sup stability of the pair  $\mathbf{V}_h, Q_h$  with help of this operator.

**Theorem 3.6.** *A projection operator  $P_h \in \mathcal{L}(\mathbf{V}, \mathbf{V}_h)$  with the property (7) and (8) implies that the finite element pair  $\mathbf{V}_h \times Q_h$  is (globally) inf-sup stable, i.e. there is a constant  $\beta > 0$ , so that for all  $q_h \in Q_h$  there exists  $\mathbf{v}_h \in \mathbf{V}_h$  with*

$$\frac{(q_h, \operatorname{div} \mathbf{v}_h)}{|\mathbf{v}_h|_1 \|q_h\|_0} \geq \beta .$$

*Proof.* Let  $q_h \in Q_h$  be given. Due to the inf-sup condition on the continuous level there exists  $\mathbf{v} \in \mathbf{V}$  with

$$\frac{(q_h, \operatorname{div} \mathbf{v})}{|\mathbf{v}|_1 \|q_h\|_0} \geq \beta_0 > 0 . \quad (10)$$

One can find a proof of this continuous inf-sup condition in Chapter I of Ref. [20], within the proof of Theorem 5.1. We choose  $\mathbf{v}_h := P_h \mathbf{v} \in \mathbf{V}_h$  and obtain

$$(q_h, \operatorname{div} \mathbf{v}_h) = (q_h, \operatorname{div} \mathbf{v}) + (q_h, \operatorname{div} (P_h \mathbf{v} - \mathbf{v})) = (q_h, \operatorname{div} \mathbf{v}) \geq \beta_0 |\mathbf{v}|_1 \|q_h\|_0 .$$

Now, we use the triangle inequality and the interpolation property (8) of  $P_h$  with  $m = 1$ :

$$|P_h \mathbf{v}|_1 \leq |P_h \mathbf{v} - \mathbf{v}|_1 + |\mathbf{v}|_1 \leq (1 + C) |\mathbf{v}|_1 .$$

The discrete inf-sup condition follows with  $\beta := \beta_0 / (1 + C)$ .  $\square$

#### 4. Local inf-sup condition for the Taylor-Hood element on anisotropic quadrilaterals

It is well-known, that the inf-sup condition plays an important role in the analysis of incompressible flows [6, 12]. Here we mention only, that in the literature one can find results on the potential dependency of the global inf-sup constant  $\beta$  on the anisotropy of the domain,  $\beta \sim (\text{aspect ratio})^{-1}$ , see [29, 17, 14, 16]. For a proof of the global discrete inf-sup condition, we refer to Ref. [13].

We are interested in an approach which takes the possible local anisotropy of the mesh into account. To this goal, we take advantage of the macro-element approach of Ref. [10], see also the presentation in [20] (Thm. II.4.2). In this section, we will prove a local inf-sup condition, as Assumption 3, for the Taylor-Hood element on anisotropic quadrilateral tensor grids. Therefore, in this section we suppose that  $\mathbf{V}_h, Q_h$  is the usual Taylor-Hood element on anisotropic quadrilateral elements in two dimensions. For an extension from 2D to 3D we refer to the techniques published by Boffi [9].

In order to find an adequate set of macro-elements  $\{M_i\}_{i=1}^R$ , we consider all interior vertices  $\sigma_i, i = 1, \dots, R$ . We define the macro-element  $M_i$  as the union of all elements  $K$  that have  $\sigma_i$  as vertex, like illustrated in Figure 1. By  $a_i$  we denote the corresponding local aspect ratio

$$a_i = \max \left\{ \frac{h_{1,K}}{h_{d,K}} : K \subset M_i \right\} .$$

For this overlapping macro-cell partition we get the following result:

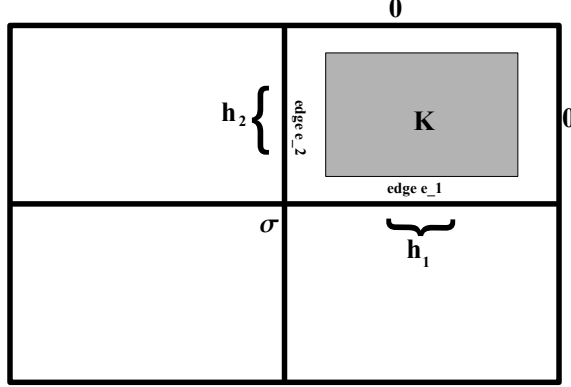


Figure 1: Illustration of a patch  $M$ .

fig:patch

thm:lbb

**Theorem 4.1.** For the  $\mathbb{Q}_2/\mathbb{Q}_1$  Taylor-Hood element on Cartesian meshes fulfilling Assumption 1 it holds the macro-element wise local inf-sup condition (6) with inf-sup constant

$$\gamma_i = C(1 + a_i^2)^{-1/2},$$

on patch  $M_i$ , i.e. Assumption 3 is fulfilled in this case.

*Proof.* Taking in mind that the variation of the local aspect ratios are bounded due to Assumption 1, the assertion is an immediate consequence of the following Lemma.  $\square$

lem:lbb

**Lemma 4.2.** Let  $\tilde{\mathbf{V}}_h \times \tilde{Q}_h$  the discrete spaces for the  $\mathbb{Q}_2/\mathbb{Q}_1$  Taylor-Hood element on a  $2 \times 2$  patch  $M = (0, 2h_1) \times (0, 2h_2)$  of quadrilaterals. Then for every  $q_h \in \tilde{Q}_h$  there exists a  $\mathbf{v}_h \in \tilde{\mathbf{V}}_h$  so that

$$(q_h, \operatorname{div} \mathbf{v}_h)_M \gtrsim \gamma_M \|q_h\|_M \|\nabla \mathbf{v}_h\|_M,$$

with  $\gamma_M := (1 + (h_1/h_2)^2)^{-1/2}$ .

*Proof.* In the following we will keep in mind the illustration of an anisotropic patch  $M$  in Figure 1. Let  $\sigma$  be the interior vertex of  $M$  and let  $\lambda$  the Lagrange  $\mathbb{Q}_1$  hat function associated to this node, i.e.,

$$\lambda(\sigma) = 1 \quad \text{and} \quad \lambda|_{\partial M} \equiv 0.$$

Hence, in the two dimensional case,  $\lambda$  vanishes on two sides of each of the four cells  $K \subset M$ . Let  $e_1, e_2$  the remaining two edges of  $K$ . The coordinate functions  $\bar{x}_i$  shall indicate the projection onto the  $x_i$ -axis but scaled with a weight  $h_i^2$ . We define  $\mathbf{v}_h$  up to some sign depending on the location of the cell within the macro-element by

$$\mathbf{v}_h(\mathbf{x}) = \left( -\frac{\partial q_h}{\partial x_1} \lambda(x_1, x_2) \bar{x}_1, -\frac{\partial q_h}{\partial x_2} \lambda(x_1, x_2) \bar{x}_2 \right),$$

where  $K$  is the corresponding cell such that  $\mathbf{x} \in K$ . Since the gradient of  $q_h$  is continuous,  $\mathbf{v}_h$  is continuous as well. This function is in  $\tilde{\mathbf{V}}_h$  since

$$\int_K \operatorname{div} \mathbf{v}_K dx = \int_{\partial K} \mathbf{v}_K \cdot \mathbf{n} ds = \int_{e_1} \mathbf{v}_K \cdot \begin{pmatrix} 0 \\ -1 \end{pmatrix} ds + \int_{e_2} \mathbf{v}_K \cdot \begin{pmatrix} -1 \\ 0 \end{pmatrix} ds = 0,$$

where we used that the first term is zero for  $x_2 = 0$  and the second for  $x_1 = 0$ .

As next step of the proof, we check the inf-sup condition. Therefore, we will prove the following statements

$$\int_M \operatorname{div} \mathbf{v}_h q_h dx = \sum_{r=1}^d \|[q_h]\|_{r,M}^2 \quad (11)$$

$$\sum_{r=1}^d \|[q_h]\|_{r,M}^2 \geq \gamma_M \|\nabla \mathbf{v}_h\|_M^2 \quad (12)$$

$$\sum_{r=1}^d \|[q_h]\|_{r,M}^2 \geq \|q_h\|_M^2, \quad (13)$$

where  $\|[q_h]\|_{r,M}$  will be defined later on. We start with

$$\int_M \operatorname{div} \mathbf{v}_h q_h dx = \sum_{K \in \mathcal{M}} \int_K \lambda \bar{x}_1 \left( \frac{\partial q_h}{\partial x_1} \right)^2 dx + \int_K \lambda \bar{x}_2 \left( \frac{\partial q_h}{\partial x_2} \right)^2 dx$$

and see that we have to integrate polynomials on each cell. Due to the construction,  $\lambda(x_1, x_2)$  is bilinear,  $\bar{x}_i$  is linear and  $\frac{\partial q_h}{\partial x_i}$  is linear in  $x_j$  where  $j \neq i$ . That is why each function in the argument of the integral is in  $\mathbb{Q}_4$ . Hence, we choose a quadrature formula which is exact for  $\mathbb{Q}_4$  functions with quadrature points  $\xi_j$  in the interior of the cell and the adequate weights  $w_j$ , for example a Gauss quadrature. With this in mind we write

$$\begin{aligned} \int_K \left( \lambda \bar{x}_1 \left( \frac{\partial q_h}{\partial x_1} \right)^2 + \lambda \bar{x}_2 \left( \frac{\partial q_h}{\partial x_2} \right)^2 \right) dx &= |K| \sum_{j=1}^k w_j \lambda(\xi_j) \left[ \bar{x}_1(\xi_j) \left( \frac{\partial q_h}{\partial x_1}(\xi_j) \right)^2 + \bar{x}_2(\xi_j) \left( \frac{\partial q_h}{\partial x_2}(\xi_j) \right)^2 \right] \\ &=: \sum_{r=1}^d \|[q_h]\|_{r,K}^2, \end{aligned}$$

and obtain (11). For showing (12) we estimate

$$\begin{aligned} \|\mathbf{v}_h\|_K^2 &\lesssim |K| \sum_{j=1}^k w_j |\mathbf{v}_h(\xi_j)|^2 \\ &= |K| \sum_{j=1}^k w_j \left[ \lambda^2(\xi_j) \bar{x}_1^2(\xi_j) \left( \frac{\partial q_h}{\partial x_1}(\xi_j) \right)^2 + \lambda^2(\xi_j) \bar{x}_2^2(\xi_j) \left( \frac{\partial q_h}{\partial x_2}(\xi_j) \right)^2 \right] \\ &\leq |K| \sum_{j=1}^k w_j \lambda(\xi_j) h_1^2 \left[ \lambda(\xi_j) \bar{x}_1(\xi_j) \left( \frac{\partial q_h}{\partial x_1}(\xi_j) \right)^2 + \lambda(\xi_j) \bar{x}_2(\xi_j) \left( \frac{\partial q_h}{\partial x_2}(\xi_j) \right)^2 \right] \\ &\leq h_1^2 \sum_{r=1}^2 \|[q_h]\|_{r,K}^2, \end{aligned}$$

where we used that  $\max_{\mathbf{x}} \lambda(\mathbf{x}) \leq 1$  and the special scaling of  $\bar{x}_i$ . The application of the inverse inequality from Remark 3.6 in Ref. [2] in every direction leads to

$$\begin{aligned} |\mathbf{v}_h|_{1,K}^2 &= \int_K \left( |\partial_{x_1} \mathbf{v}_h|^2 + |\partial_{x_2} \mathbf{v}_h|^2 \right) dx \\ &\leq h_1^{-2} \|\mathbf{v}_h\|_K^2 + h_2^{-2} \|\mathbf{v}_h\|_K^2 \\ &= \frac{h_1^2 + h_2^2}{h_1^2 h_2^2} \|\mathbf{v}_h\|_K^2. \end{aligned}$$

These two estimates together give (12) with  $\text{leq:infsupzz2}$

$$\gamma_M := \min_{K \in M} \frac{h_2}{\sqrt{h_1^2 + h_2^2}} = \frac{1}{\sqrt{a_i^2 + 1}},$$

and where  $a_i = \max_{K \in M} \frac{h_1}{h_2}$ . (The  $i$  denotes the  $i$ -th macro-element in set of macro-elements later on for Theorem 4.1.) Now it is left to show the statement (13):  $\text{thm:1bb}$   $\text{eq:infsupzz3}$

$$\begin{aligned} \|q_h\|_{0,M}^2 &= \sum_{K \in M} \|q_h\|_{0,K}^2 \\ &\leq \sum_{K \in M} h_1^2 \left\| \frac{\partial q_h}{\partial x_1} \right\|_K^2 + h_2^2 \left\| \frac{\partial q_h}{\partial x_2} \right\|_K^2 \\ &\leq \sum_{K \in M} \left( \min_{i=1,2} \min_{j=1,\dots,k} (\lambda(\xi_j) h_i^{-2} \bar{x}_i(\xi_j)) \right)^{-1} |K| \sum_{i=1}^2 \sum_{j=1}^k w_j h_i^2 \lambda(\xi_j) h_i^{-2} \bar{x}_i(\xi_j) \left( \frac{\partial q_h}{\partial x_i}(\xi_j) \right)^2 \\ &\leq \sum_{K \in M} |K| \sum_{j=1}^k w_j \left[ \lambda(\xi_j) \bar{x}_1(\xi_j) \left( \frac{\partial q_h}{\partial x_1}(\xi_j) \right)^2 + \lambda(\xi_j) \bar{x}_2(\xi_j) \left( \frac{\partial q_h}{\partial x_2}(\xi_j) \right)^2 \right] \\ &= \sum_{r=1}^2 \|[q_h]\|_{r,M}^2, \end{aligned}$$

where we used the variant of Poincaré's inequality from Lemma 2.2, the Definition 1 of the mesh and the special choice of  $\bar{x}_i$  in the definition of  $\mathbf{v}_h$  at the beginning. This proves to claim.  $\square$   $\text{lem:poincare}$   $\text{ass:1}$

Now we can choose a mesh with respect to Assumption 1 and 2 and the  $\mathbb{Q}_2/\mathbb{Q}_1$  Taylor-Hood element. Then due to Theorem 4.1 Assumption 3 is fulfilled also and we can apply Theorem 3.5 to obtain the following.  $\text{thm:1bb}$   $\text{ass:3}$   $\text{thm:main}$

**Corollary 4.3.** *Under the assumptions from above there exists an operator  $P_h \in \mathcal{L}(\mathbf{V}, \mathbf{V}_h)$  with the properties (7) and (8).*  $\text{cor:anisoop}$   $\text{eq:dipromzinterpol}$

## 5. Discussion on Assumption 2 $\text{ass:2}$

The Assumption 2 implies that the assignment of inner long edges for each  $K$  is possible in an injective manner. This is a certain restriction on the mesh and not always valid in the case of Dirichlet conditions. For illustration we consider two standard examples.  $\text{sec:assert}$   $\text{ass:2}$

### 5.1. Channel flow $\text{sec:channel}$

A channel flow is usually characterized by Dirichlet conditions at solid walls and sometimes also at the inflow. The outflow is typically considered as “do-nothing” condition [22]. At high Reynolds numbers, the mesh size close to the walls should be anisotropic with a small mesh size in direction orthogonal to the walls. For the definition of  $\varepsilon_h$  in Assumption 2 we choose the inner long edge  $\varepsilon_h(K)$  starting from a boundary cell  $K$  of the two no-slip walls. This procedure is shown schematically in Figure 2 (a) where the arrows in the figure point from the cell to the chosen edge. We continue this process by choosing successively the longer edges towards the center of the channel. At the center we have to choose an edge in direction towards the outflow in order to maintain injectivity of  $\varepsilon_h$ . For at least one cell we reach the outflow boundary. Hence, the cells at the center should be (almost) isotropic for this algorithm. If the outflow boundary is not of Dirichlet type, the operator may not preserve this condition.  $\text{fig:edge}$   $\text{fig:woodkannacherlurek92}$

(a) (b)

Figure 2: Examples of how to choose a long edge for a cell  $K$  in Assumption 2. The arrows on a cell  $K$  reference to the assigned edge  $\varepsilon_h(K)$ : (a): configuration of channel-type (Section 5.1), (b): driven cavity with Dirichlet conditions on the entire boundary (Section 5.2).

### 5.2. Driven cavity flow

For the standard driven cavity problem (here in 2D), Dirichlet conditions are posed on the entire boundary. Therefore, the construction as before in the channel with outflow boundary is not possible. We assume anisotropic cells on all four boundaries with small mesh sizes in normal direction. At the corners the cells are isotropic, see Figure 2 (b). The construction of  $\varepsilon_h$  can be carried out by assigning long edges as shown schematically in Figure 2 (b). Let us point out that for this type of meshes Assumption 1 is not fulfilled, since there is not only one direction with small edges. This Assumption is important especially in the proof of Lemma 4.2, where we use the geometry with one smaller edges. To extend the proof to meshes like in Figure 2 (b), we can simply rotate the patches and use the same arguments to obtain the assertion.

## 6. Application to incompressible flow problems

In this section, we will discuss the applicability of theoretical results to (turbulent) incompressible flow problems in a bounded domain  $\Omega \subseteq \mathbb{R}^d, d \in \{2,3\}$  if the standard Taylor-Hood pairs for velocity/pressure approximation are applied on tensor-product meshes.

The incompressible Navier-Stokes model consists in determining velocity  $\mathbf{u}$  and pressure  $p$  s.t.

$$\partial_t \mathbf{u} - \operatorname{div}(2\nu \mathbb{D}\mathbf{u}) + (\mathbf{u} \cdot \nabla)\mathbf{u} + \nabla p = \mathbf{f} \quad \text{in } (0, T] \times \Omega \quad (14)$$

$$\operatorname{div} \mathbf{u} = 0 \quad \text{in } [0, T] \times \Omega \quad (15)$$

$$\mathbf{u}|_{t=0} = \mathbf{u}^0 \quad \text{in } \Omega. \quad (16)$$

The deformation tensor is denoted by  $\mathbb{D}\mathbf{u} = \frac{1}{2}(\nabla\mathbf{u} + (\nabla\mathbf{u})^t)$ . For simplicity, we consider no-slip boundary conditions and thus, for a weak formulation, the spaces  $\mathbf{V} = [H_0^1(\Omega)]^d, Q = L_*^2(\Omega)$ , see Section 1.

Let  $\mathbb{T}_h$  be an admissible (possibly anisotropic) mesh s.t.  $\bar{\Omega} = \cup_{K \in \mathbb{T}_h} \bar{K}$ . We consider the standard inf-sup stable Taylor-Hood spaces  $\mathbf{V}_h \times Q_h \subset \mathbf{V} \times Q$  for velocity/pressure. The basic Galerkin FE method reads: find  $(\mathbf{u}_h, p_h) : [0, T] \rightarrow \mathbf{V}_h \times Q_h$  s.t.  $\forall (\mathbf{v}_h, q_h) \in \mathbf{V}_h \times Q_h$

$$(\partial_t \mathbf{u}_h, \mathbf{v}_h) + (2\nu \mathbb{D}\mathbf{u}_h, \mathbb{D}\mathbf{v}_h) + b_S(\mathbf{u}_h, \mathbf{u}_h, \mathbf{v}_h) - (p_h, \operatorname{div} \mathbf{v}_h) + (q_h, \operatorname{div} \mathbf{u}_h) = (\mathbf{f}, \mathbf{v}_h)$$

with the skew-symmetric advective term  $b_S(\mathbf{u}, \mathbf{v}, \mathbf{w}) := \frac{1}{2}[(\mathbf{u} \cdot \nabla)\mathbf{v}, \mathbf{w}] - ((\mathbf{u} \cdot \nabla)\mathbf{w}, \mathbf{v})$ .

For turbulent flows, we consider the following three-scale decomposition

$$\mathbf{V} \ni \mathbf{v} = \underbrace{\bar{\mathbf{v}}_h + \tilde{\mathbf{v}}_h}_{=\mathbf{v}_h \in \mathbf{V}_h} + \hat{\mathbf{v}}_h; \quad Q \ni q = \underbrace{\bar{q}_h + \tilde{q}_h}_{=q_h \in Q_h} + \hat{q}_h$$

with resolved scales  $(\mathbf{v}_h, q_h) \in \mathbf{V}_h \times Q_h \subset \mathbf{V} \times Q$ . The influence of the small unresolved scales  $(\hat{\mathbf{v}}_h, \hat{q}_h)$  on  $(\tilde{\mathbf{v}}_h, \tilde{q}_h)$  will be modelled following the one-level variational multiscale (VMS) approach, see [8]. Define the discontinuous space  $L_h$  for the deformation tensor on  $\mathbb{T}_h$  s.t.

$$\{0\} \subseteq L_h \subseteq L := \{\mathbf{L} = (l_{ij}) \mid l_{ij} = l_{ji} \in L^2(\Omega) \forall i, j \in \{1, 2, 3\}\}$$

and the  $L^2$ -orthogonal projection operator  $\Pi_h : L \rightarrow L_h$ . The small unresolved velocity scales are modelled via the fluctuation operator

$$\kappa(\mathbb{D}\mathbf{v}_h) := (Id - \Pi_h)(\mathbb{D}\mathbf{v}_h).$$

For the calibration of the subgrid model for velocity, we introduce cellwise constant terms  $\nu_T(\mathbf{u}_h)$  s.t.  $\nu_T^K(\mathbf{u}_h) := \nu_T(\mathbf{u}_h)|_K$ . Here we omit a model of the small unresolved pressure scales by means of the so-called grad-div stabilization. Finally, the VMS model reads as follows: find  $(\mathbf{u}_h, p_h)$  s.t.

$$\begin{aligned} (\partial_t \mathbf{u}_h, \mathbf{v}_h) + 2\nu(\mathbb{D}\mathbf{u}_h, \mathbb{D}\mathbf{v}_h) + b_S(\mathbf{u}_h, \mathbf{u}_h, \mathbf{v}_h) + (\operatorname{div} \mathbf{u}_h, q_h) - (\operatorname{div} \mathbf{v}_h, p_h) \\ + (\nu_T(\mathbf{u}_h)\kappa(\mathbb{D}\mathbf{u}_h), \kappa(\mathbb{D}\mathbf{v}_h)) = (\mathbf{f}, \mathbf{v}_h) \end{aligned} \quad (17) \quad \text{eq:VMS}$$

for all  $(\mathbf{v}_h, q_h) \in \mathbf{V}_h \times Q_h$ .

For the analysis, we introduce elementwise multiscale viscosities  $\nu_{\text{VMS}}^K(\mathbf{u}_h, \mathbf{v}_h)$  via

$$\sum_{K \in \mathbb{T}_h} \nu_T^K(\mathbf{u}_h) \|\kappa(\mathbb{D}\mathbf{v}_h)\|_{0,K}^2 = \sum_{K \in \mathbb{T}_h} \underbrace{\nu_T^K(\mathbf{u}_h) \left(1 - \frac{\|\Pi_H \mathbb{D}\mathbf{v}_h\|_{0,K}^2}{\|\mathbb{D}\mathbf{v}_h\|_{0,K}^2}\right)}_{=: \nu_{\text{VMS}}^K(\mathbf{u}_h, \mathbf{v}_h) \geq 0} \|\mathbb{D}\mathbf{v}_h\|_{0,K}^2$$

where we take advantage of the projector properties of the operator  $\kappa$ . Then we define the mesh-dependent expression

$$\|\|\mathbf{u}(t)\|\|^2 := \|\mathbf{u}(t)\|_0^2 + \sum_{K \in \mathbb{T}_h} \int_0^t \frac{1}{2} \nu_{\text{mod}}^K(\mathbf{u}, \mathbf{u}_h) \|\mathbb{D}(\mathbf{u})\|_{0,K}^2 dt$$

with modified elementwise viscosities:  $\nu_{\text{mod}}^K(\mathbf{u}_h, \mathbf{v}_h) := 2\nu + \nu_{\text{VMS}}^K(\mathbf{u}_h, \mathbf{v}_h)$ .

The semi-discrete analysis in [26] takes advantage of the fact that, for inf-sup stable velocity/pressure pairs, the space

$$\mathbf{V}_h^{\text{div}} := \{\mathbf{v} \in \mathbf{V}_h : (q_h, \operatorname{div} \mathbf{v}_h) = 0 \ \forall q_h \in Q_h\}$$

of discretely divergence free functions is not empty. Then we obtain the following a priori estimate for the semi-discrete scheme.

thm:vms

**Theorem 6.1.** *For a sufficiently smooth solution  $\mathbf{u}$  of the Navier-Stokes model (14)-(16) it holds for the solution of the VMS model (17) for all  $t \in (0, T)$ :*

$$\begin{aligned} \|\|\mathbf{u} - \mathbf{u}_h(t)\|\|^2 \leq 2 \inf_{\tilde{\mathbf{u}}_h \in L^2(0, t; \mathbf{V}_h^{\text{div}})} \|\|\mathbf{u} - \tilde{\mathbf{u}}_h(t)\|\|^2 \\ + \exp\left(\int_0^t \frac{27C_{LT}^4}{2\nu_{\text{mod}}^{\min}(\mathbf{u}_h, \mathbf{e}_h^u)^3} ds\right) \|\mathbb{D}\mathbf{u}(s)\|_0^4 ds \inf_{\substack{\tilde{\mathbf{u}}_h \in L^4(0, t; \mathbf{V}_h^{\text{div}}) \\ \tilde{p}_h \in L^2(0, t; Q_h)}} \left( \|\mathbf{u}_h - \tilde{\mathbf{u}}_h(0)\|_0^2 + \int_0^t A(s) ds \right) \end{aligned}$$

with

$$\begin{aligned} A(t) := & 2 \sum_{K \in \mathbb{T}_h} \left[ 6\nu_T^K(\mathbf{u}_h) \|\kappa \mathbb{D}\mathbf{u}\|_{0,K}^2 + 6\left(\nu + \nu_{\text{VMS}}^K(\mathbf{u}_h, \epsilon^u)\right) \|\mathbb{D}\epsilon^u\|_{0,K}^2 + \frac{9C_{Ko}^2}{\nu_{\text{mod}}^{\min}(\mathbf{u}_h, \mathbf{e}_h^u)} \|p - \tilde{p}_h\|_{0,K}^2 \right] \\ & + \frac{6C_{LT}^2}{\nu_{\text{mod}}^{\min}(\mathbf{u}_h, \mathbf{e}_h^u)} \left( C_F C_{Ko} \|\mathbb{D}\mathbf{u}\|_0^2 + \|\mathbf{u}_h\|_0 \|\mathbb{D}\mathbf{u}_h\|_0 \right) \|\mathbb{D}\epsilon^u\|_0^2 + \frac{6C_{Ko}^2}{\nu_{\text{mod}}^{\min}(\mathbf{u}_h, \mathbf{e}_h^u)} \|\partial_t \epsilon^u\|_{-1, \Omega}^2, \end{aligned}$$

where  $\nu_{\text{mod}}^{\min}(\mathbf{u}_h, \mathbf{e}_h^u) := \min_K \nu_{\text{mod}}^K(\mathbf{u}_h(t), \mathbf{v}_h(t))$  and

$$\mathbf{u}_h - \mathbf{u} = (\mathbf{u}_h - \tilde{\mathbf{u}}_h) - (\mathbf{u} - \tilde{\mathbf{u}}_h) =: \mathbf{e}_h^u - \epsilon^u.$$

$C_F$  and  $C_{Ko}$  are the constants of the inequalities of Friedrichs and Korn.  $C_{LT}$  is related to an upper bound of the advective term.

**Remark 6.2.** Let us briefly review the case of isotropic grids considered in [26]. The first r.h.s. term in the first line of term  $A(t)$  is related to the VMS-model error. For the remaining approximation terms in  $A$ , we can apply the interpolation operator by Girault/Scott [21] in  $\mathbf{V}_h^{div}$  and a standard interpolation operator for the pressure. Then these terms are formally of order  $\mathcal{O}(h^{2k})$  for FE spaces  $\mathbb{Q}_k/\mathbb{Q}_{k-1}$  or  $\mathbb{P}_k/\mathbb{P}_{k-1}$  for velocity/pressure, the choice  $L_H = [\mathbb{Q}_{k-2}^{disc}]^{3 \times 3}$ , and  $\nu_T^K \in [0, Ch_K^2]$ .

### 6.1. Isothermal channel flow

Suppose now a tensor-product mesh  $\mathbb{T}_h$  on a channel domain  $\Omega = (0, 4\pi) \times (-H, H) \times (0, \frac{4}{3}\pi)$ . Then we can apply the results of Theorem 3.5 to the evaluation of the right-hand side terms in the function space  $\mathbf{V}_h^{div}$  in Theorem 6.1.

Consider now a turbulent flow at a moderate Reynolds number  $Re_\tau = 180$  (corresponding to  $Re = 5644$  in channel center) for which an anisotropic grid resolution of the boundary layer regions is feasible. The Reynolds number  $Re_\tau = Hu_\tau/\nu$  is defined via the half width  $H = 1$  of the channel and wall-friction velocity  $u_\tau$  satisfying Spalding's form of the law of the wall

$$y^+ = f(u^+) := u^+ + e^{-5.5\chi} \left( e^{\chi u^+} - 1 - \chi u^+ - \frac{1}{2}(\chi u^+)^2 - \frac{1}{6}(\chi u^+)^3 \right)$$

with  $y^+ := \frac{yu_\tau}{\nu}$ ,  $u^+ := \frac{\|\mathbf{u}_h\|}{u_\tau}$ , and  $\chi = 0.4$ .

A careful description of the set-up of the problem (but with different scaling) is given in [23]. For the spatial discretization, we apply tensor-product hexahedral meshes with FE spaces  $\mathbb{Q}_2/\mathbb{Q}_1$  for velocity/pressure within the FE package deal.II, see [7]. The viscosity model is given by

$$\nu_T(\mathbb{D}\mathbf{u}_h)\kappa(\mathbb{D}\mathbf{u}_h).$$

with the fluctuation operator  $\kappa := Id - \Pi_h$ , the  $L^2$ -orthogonal projection  $\Pi_h : L \rightarrow L_h$ , and  $L_h = \mathbb{Q}_0^{d \times d}$  together with a model close to the classical Smagorinsky

$$\nu_T(\mathbb{D}\mathbf{u}_h)|_K = (C_S \Delta_K)^2 \|\kappa \mathbb{D}\mathbf{u}_h(S_K)\|_F.$$

Here,  $S_K$  denotes the center of gravity of element  $K$ . On each element  $K \in \mathbb{T}_h$ , the filter width is given by the geometric mean of the cell  $\Delta_K = (\text{meas}(K))^{1/d}$ . The model parameter  $C_S^2 = 0.2010$  is taken from Lilly's argument for isotropic homogeneous turbulence, see [26].

We performed simulations with  $16 \times 24 \times 16$  grid points, with equidistant distribution of elements in  $x_1, x_3$ -directions and anisotropic distribution in  $x_2$ -direction according to

$$x_2 = y = \tanh(2(2i/(N) - 1))/\tanh(2), \quad \text{for } i = 0, \dots, N.$$

For this mesh, illustrated in Figure 3, we obtained a value of the aspect ratio  $\alpha_\Omega \approx 25$ .

Statistical averaging  $\langle \cdot \rangle$  is performed over all homogeneous directions  $x_1, x_3, t$ . As an example of first-order statistics, we present in Fig. 4 the mean streamwise velocity  $U = \langle \mathbf{u}_h \rangle \cdot \mathbf{e}_1$  and its normalized variant  $U^+$ . Compared to direct numerical simulation (DNS) results of [25], we obtain very good agreement in the viscous sub-layer whereas slight deviations can be found in the log-layer and in the center of the channel.

**Remark 6.3.** An anisotropic resolution of boundary layers seems reasonable for moderate Reynolds numbers  $Re_\tau$ , but becomes much more expensive with increasing  $Re_\tau$ . Moreover, the applicability of our anisotropic estimates in Theorem 3.5 becomes questionable with very large aspect ratio. Numerical experiments in [4] with lowest-order Taylor-Hood elements on anisotropic grids show indeed a potential influence of a large aspect ratio  $\alpha_\Omega := \max_K h_K/\rho_K$  where  $h_K$  and  $\rho_K$  denote the diameter of  $K$  resp. the diameter of the largest ball in  $K$ . A remedy is the application of wall-functions for high  $Re_\tau$ .

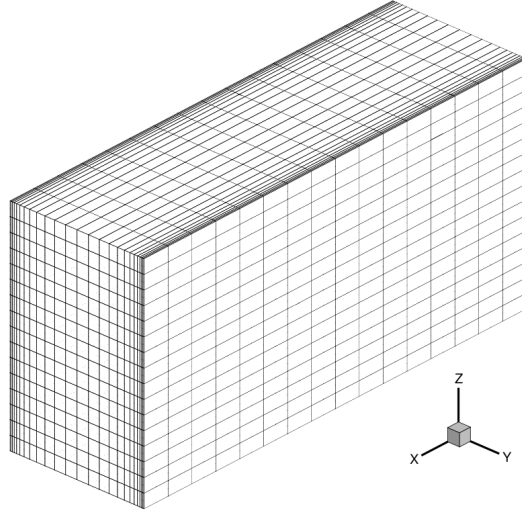


Figure 3: Mesh for the Channel flow with  $16 \times 24 \times 16$  grid points, fitting into the framework of Assumption 2. ass:2

fig:cmesh

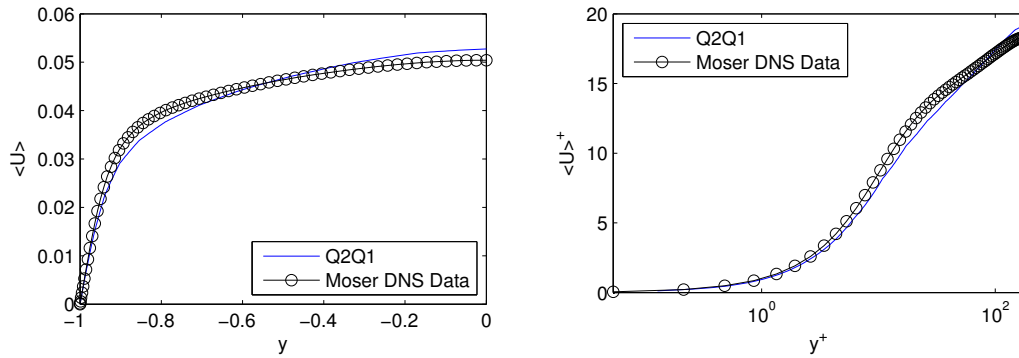


Figure 4: Channel flow at  $Re_\tau = 180$  with  $16 \times 24 \times 16$  grid points: Mean streamwise velocity  $U = \langle \mathbf{u}_h \rangle \vec{e}_1$  (left) and its normalized variant  $U^+ = U/u_\tau$  (right)

fig:1

## 6.2. Non-isothermal cavity flow

Finally, we demonstrate the applicability of our approach to non-isothermal flow in a cavity. To this goal we expand model (14)-(16) by adding the Fourier model

$$\partial_t \theta - \kappa \Delta \theta + \mathbf{u} \cdot \nabla \theta = Q \quad (18)$$

for temperature  $\theta$  and setting  $\mathbf{f} = \alpha \mathbf{g} \theta$  in (14). The Galerkin formulation of (18) takes advantage of a skew-symmetric form of the advective term. Moreover, a variational multiscale stabilization of the temperature is introduced according to Subsec. 6.1. For more details, we refer to [24] where an extension of Theorem 6.1 to the Navier-Stokes/Fourier model (14)-(16), (18) is given as well.

Exemplarily, we apply the method to natural convection in a differentially heated cavity  $\Omega := (0, 1)^2$ . Heating  $\theta = \theta_{max}$  and cooling  $\theta = \theta_{min}$  is performed at lateral boundaries, whereas the upper and lower boundaries are highly conducting. No-slip conditions  $\mathbf{u} = \mathbf{0}$  for velocity are given at the whole boundary  $\partial\Omega$ . Strong boundary layers for temperature (and velocity) appear on the lateral boundaries, see Fig. 5 (right).

Computations were done on with  $Q_2/Q_1/Q_2$  elements for velocity, pressure, and temperature on two meshes with 64 and 32 cells in each dimension. An anisotropic mesh refinement had been performed at all



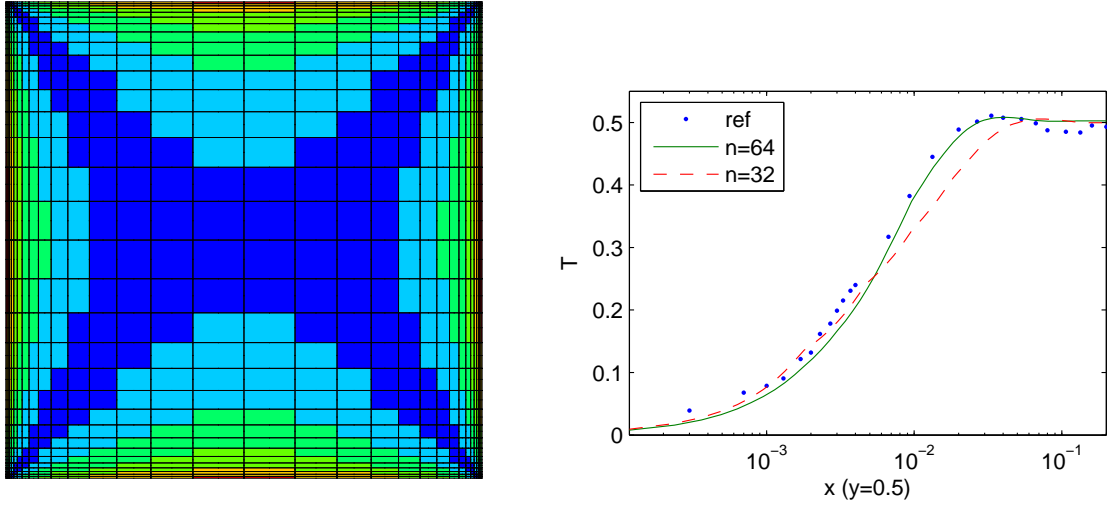


Figure 5: Anisotropic tensor-product mesh on a cavity (left); Boundary layer profile for temperature profile  $T(x, 0.5)$  and experimental data [28] (right)

fig:4

boundaries by transforming an equidistant reference mesh with

$$x_1 = \hat{x}_1 - \frac{19}{40\pi} \sin(2\pi\hat{x}_1), \quad x_2 = \hat{x}_2 - \frac{7}{16\pi} \sin(2\pi\hat{x}_2).$$

The maximum aspect-ratio of cells at the vertical walls was about 36:1, see Fig. 5 (right). It is possible to show that Assumption 2 is valid for such mesh too.

Results for time-averaged quantities of a low-turbulence flow at  $Ra = 1.58 \times 10^9$  are shown in Fig. 5 (right). Here we used the projection-based VMS with a Smagorinsky-Eidson parametrization of the subgrid model. On the fine grid, we observe a good agreement with the experimental data in [28].

**Remark 6.4.** Let us finally remark that Remark 6.3 remains valid for this application as well.

## 7. Conclusion

Summarizing, we conclude that under the Assumptions 1, 2 and 3 there exists an anisotropic interpolation operator, which preserves the discrete divergence (3). This was proven in Theorem 3.5. Moreover, in 2 dimensions the Taylor-Hood element  $\mathbb{Q}_2/\mathbb{Q}_1$  fulfills Assumption 3 and we get the existence of an interpolation operator in this case from Corollary 4.3 (with respect to the local aspect ratio). Further the numerical tests in Section 6 showed good results on anisotropic meshes for complex benchmark problems, i.e. a channel flow and a cavity flow.

## Acknowledgment

We would like to thank Timo Heister for supporting the parallel computations presented in Subsec. 6.1 and Johannes Löwe for providing the numerical results for Subsec. 6.2. The research of Lars Röhe was supported by the German Research Foundation (DFG) through Research Training Group GK 1023.

- [1] T. APEL, *Interpolation of non-smooth functions on anisotropic finite element meshes*, M2AN, 33 (1999), pp. 1149–1185.
- [2] T. APEL AND G. LUBE, *Anisotropic mesh refinement for singularly perturbed reaction diffusion problems*, Preprint TU Chemnitz-Zwickau, SFB393/96-11 (1996), pp. 1–25.
- [3] T. APEL AND G. MATTHIES, *Non-conforming, anisotropic, rectangular finite elements of arbitrary order for the Stokes problem*, SIAM J. Numer. Anal., 46 (2008), pp. 1867–1891.

- Apel03 [4] T. APEL AND H. RANDRIANARIVONY, *Stability of discretizations of the stokes problem on anisotropic meshes*, Math. Comput. Simulation, 61 (2003), pp. 437–447.
- apel20082 [5] T. APEL AND D. SIRCH,  *$L_2$ -error estimates for the Dirichlet and Neumann problem on anisotropic finite element meshes*, Preprint SPP1253-02-05 (2008), (2008).
- babuska [6] I. BABUŠKA, *The Finite Element Method with Lagrangian Multipliers*, Num. Math., 20 (1973), pp. 179–192.
- dealdesc [7] W. BANGERTH, R. HARTMANN, AND G. KANSCHAT, *deal.II — a General Purpose Object Oriented Finite Element Library*, ACM Trans. Math. Software, 33 (2007). article 24.
- BIL06 [8] L. BERSELLI, T. ILIESCU, AND W. LAYTON, *Mathematics of Large Eddy Simulation of Turbulent Flows*, Springer, Berlin, Heidelberg, 2006.
- boffi97 [9] D. BOFFI, *Three-dimensional finite element methods for the Stokes problem*, SIAM J. Numer. Anal., (1997), pp. 664–670.
- nikolaides83 [10] J. BOLAND AND R. NICOLAIDES, *Stability of finite elements under divergence constraints*, SIAM J. Numer. Anal., 20 (1983), pp. 722–731.
- Braack08 [11] M. BRAACK, *A stabilized finite element scheme for the navier-stokes equations on quadrilateral anisotropic meshes*, M2AN, 42 (2008), pp. 903–924.
- brezzi [12] F. BREZZI, *On the Existence, Uniqueness and Approximation of Saddle-Point Problems Arising from Lagrangian Multipliers*, R.A.I.R.O., Anal. Numer., 8 R2 (1974), pp. 129–151.
- brezziFalk91 [13] F. BREZZI AND R. FALK, *Stability of higher-order hood-taylor methods*, SIAM J. Numer. Anal., 28 (1991), pp. 581–590.
- zhonkov2000 [14] E. CHIZHONKOV AND M. OLSHANSKII, *On the domain geometry dependence of the LBB condition*, Mathematical Modelling and Numerical Analysis, 34 (2000), pp. 935–951.
- ciarlet78 [15] P. CIARLET, *The Finite Element Method for Elliptic Problems*, North-Holland, Amsterdam, New York, Oxford, 1978.
- lski2003lbb [16] M. DOBROWOLSKI, *On the LBB constant on stretched domains*, Mathematische Nachrichten, 254 (2003), pp. 64–67.
- dob2005lbb [17] ———, *On the LBB condition in the numerical analysis of the Stokes equations*, Applied Numerical Mathematics, 54 (2005), pp. 314–323.
- dziuk [18] G. DZIUK, *Theorie und Numerik Partieller Differentialgleichungen*, de Gruyter, Berlin, New York, 2010.
- Formaggia04 [19] L. FORMAGGIA, S. MICHELETTI, AND S. PEROTTO, *Anisotropic mesh adaptation in computational fluid dynamics: Application to the advection-diffusion-reaction and the Stokes problems\* 1*, Applied Numerical Mathematics, 51 (2004), pp. 511–533.
- gr [20] V. GIRAULT AND P.-A. RAVIART, *Finite Element Methods for Navier-Stokes Equations*, Springer, Berlin, 1986.
- interpolgir [21] V. GIRAULT AND L. SCOTT, *A quasi-local interpolation operator preserving the discrete divergence*, Calcolo, 40 (2003), pp. 1–19.
- cherTurek92 [22] J. HEYWOOD, R. RANNACHER, AND S. TUREK, *Artificial boundaries and flux and pressure conditions for the incompressible Navier-Stokes equations*, Int. J. Numer. Meth. Fluids., 22 (1996), pp. 325–352.
- ohnRoland07 [23] V. JOHN AND M. ROLAND, *Simulations of the turbulent channel flow at  $re_\tau = 180$  with projection-based finite element variational multiscale methods*, Int. J. Numer. Meth. Fluids, 55 (2007), pp. 407–429.
- LLR10 [24] J. LÖWE, G. LUBE, AND L. RÖHE, *A Projection-based Variational Multiscale Method for the Incompressible Navier-Stokes/Fourier Model*, in LNCS BAIL (to appear), 2010.
- Moser99 [25] R. MOSER, J. KIM, AND N. MANSOUR, *Direct numerical simulation of turbulent channel flow up to  $Re_\tau = 590$* , Physics of Fluids, 11 (1999), pp. 943–945.
- RL10 [26] L. RÖHE AND G. LUBE, *Analysis of a variational multiscale method for Large-Eddy simulation and its application to homogeneous isotropic turbulence*, Comp. Meth. Appl. Mech. Engrg., 199 (2010), pp. 2331–2342.
- lscottzhang [27] L. SCOTT AND S. ZHANG, *Finite Element Interpolation of Nonsmooth Functions Satisfying Boundary Conditions*, Math. Comp., 54 (1990), pp. 483–493.
- TianKara00 [28] Y. TIAN AND T. KARAYIANNIS, *Low turbulence natural convection in an air filled square cavity. Part I: the thermal and fluid flow fields*, Int. J. Heat Mass Transfer, 43 (1000), pp. 849–866.
- rowowski08 [29] M. WOHLMUTH AND M. DOBROWOLSKI, *Numerical analysis of stokes equations with improved LBB dependency*, Electronic Transactions on Numerical Analysis, 32 (2008), pp. 173–189.